Tikrit Journal of Engineering Sciences/Vol.19/No.1/March 2012, (14-22)

Bearing Capacity of Eccentrically Loaded Strip Footing on Geogrid Reinforced Sand

Dr. Jawdat K. Al-Tirkity — **Assist. Prof.**
Akram H. Al-Taay — **Engineer**
Civil Eng. Dept., University of Tikrit

Abstract
This study aims to demonstrate the effects of geogrid reinforcement on the bearing capacity of strip footing under eccentric loading. Numerical analysis using finite element program called (PLAXIS 2D Professional v.8.2) are presented. The effect of each of the depth ratio of the topmost layer of geogrid (u/B), the vertical distance ratio between consecutive layers (h/B), number of geogrid layers (N), and the effective depth ratio of reinforcement (d/B) on the bearing capacity were studied, where (B) is the footing width. Also, the combined effect of load eccentricity ratio (e/B), depth of embedment ratio of footing (D_f/B) and the angle of internal friction (ϕ) on the ultimate bearing capacity were investigated.
Keywords: Bearing Capacity, Eccentric load, Finite element method, Geogrid, Reinforced Sand, Strip Footing.

قابلية التحمل لأساس شريطي محمل لامركزياً على تربة رملية مسلحة

الخلاصة
تهدف هذه الدراسة إلى إظهار تأثير التسليح على قابلية التحمل لأساس شريطي تحت تأثير حمل لا مركزي. قدمت نتائج التحليل العددي لبرنامج للعناصر المحددة يدعى (PLAXIS 2D Professional v.8.2). تم دراسة تأثير نسبة عمق الدفن لأول طبقة من التسليح (u/B) ونسبة المسافة العمودية بين طبقات التسليح (h/B) وعدد طبقات التسليح (N) ونسبة العمق الفعال لطبقات التسليح (d/B) على قابلية التحمل، حيث (B) هي عرض الأساس، ومن ثم دراسة التأثير المركب لنسبة اللامركزية في الحمل (e/B) ونسبة عمق الدفن للأساس (D_f/B) وأيضا زاوية الاحتكاك الداخلي (ϕ) للتربة على قابلية التحمل القصوى.
الكلمات الدالة : أساس شريطي، تربة مسلحة، اللامركزية، العناصر المحددة، قابلية التحمل.

Notations

B : width of the footing.
BCR_e : bearing capacity ratio.
c : soil cohesion.
d : effective depth of reinforcement.
D_f : Depth of footing base below the ground surface.
e : load eccentricity.
E_{50} : Modulus of elasticity.
EA : normal stiffness.
EI : flexural rigidity .
h : vertical distance between consecutive layers of reinforcement.
N: number of reinforcement layers.
q_{uRe} : Ultimate bearing capacity of eccentrically loaded strip footing on reinforced sand.
q_u : Ultimate bearing capacity of centrically loaded strip footing on unreinforced sand.
R_{int} : interface reduction factor
u : depth of first layer of reinforcement below the footing base.
ϕ : Angle of internal friction of sand.
ψ : Angle of dilatancy.
γ : Unit weight of the soil.
ν : Poisson's ratio

Introduction

The load eccentricity significantly reduces the bearing capacity of the supporting soil by tilting the footing and heaving the supporting soil. This might be avoided either by constructing the footing with larger dimensions to reduce the contact pressure which leads to uneconomical design or by increasing the bearing capacity of the supporting soil. (El Sawwaf 2009)[1]

The behavior of eccentrically loaded strip footing on unreinforced sand has been reported by several researchers such as Meyerhof (1953)[2] proposed the equivalent area method or the effective width method, Prakash and Saran (1971)[3] provided a comprehensive mathematical formulation to estimate the ultimate bearing capacity of a rough strip foundation under eccentric loading and Purkayastha and Char (1977)[4] proposed a reduction factor to estimate the ultimate bearing capacity of eccentrically loaded strip footing.

Several studies have reported the successful use of soil reinforcement as a cost-effective method to increase the ultimate bearing capacity at a given settlement under shallow foundations such as (Binquet and Lee (1975)[5&6], Huang and Tatsuoka (1990)[7], Das and Omar (1994)[8], Adams and Collin (1997)[9], Huang and Menq (1997)[10], Shin and Das (2000)[11] and Saran et al. (2007)[12]). This was achieved by removing the existing weak soil up to a certain depth and then replacing the soil or fills the same soil back with inclusion of horizontal layers of geosynthetic at different depths under the footing. Therefore, with the potential benefit of using soil reinforcement both the type and the size of foundation may be changed leading to an economic design. However, few studies have been concentrated on the behavior of eccentrically loaded strip footing supported on reinforced sand. Patra et al. (2006)[13] reported the results of a laboratory small-scale model tests for eccentrically loaded strip footing on geogrid reinforced sand. Also El-Sawwaf (2009)[1] studied numerically and experimentally the ultimate bearing capacity of eccentrically loaded surface strip footing on geogrid reinforced sand where particular attention was given to simulate footing constructed on unsymmetrical geogrid layers with eccentricity on either direction of the footing. It should be mentioned that these studies covered only some of the controlling parameters of the problem. Therefore, the main aim of this research is to cover most of the parameters related. i.e. studying the combined effect of load eccentricity along with the depth of footing and the angle of internal friction for most of the reinforcement parameters on the ultimate bearing capacity.

Finite Element Formulation and Material Modeling

The nonlinear behavior of sand was modeled using Mohr-Coulomb soil model, which is an elastic perfect-plastic stress-strain model; the footing was treated as elastic beam elements with significant flexural rigidity (*EI*) and normal stiffness (*EA*). Interface elements have been used to model both the interaction between the footing base and the soil and the interaction between the geogrid and soil from both sides. The interface elements allow for the specification of a reduced wall friction compared to the friction of the soil. Automatic generation of (15 node) triangle plane strain elements for the soil, (5 node) beam elements for the footing and (5 node) elastic line elements for the geogrid were used. The soil parameters used in the present study are listed in Table (1), the footing and

geogrid parameters are listed in Table (2) and the engineering properties of the geogrid are the same that listed in Table (3). For more details about the elements types, formulation and the parameters used refer to (Al-Taay 2010)[14].

The Studied Parameters

Since the soil can not sustain tension stresses which mostly happen when the eccentricity ratio (e/B) increases more than (1/6). The eccentricity ratios (e/B) in the present study were varied (from 0 to 0.15), the depth ratio of footing embedment (D_f /B) were varied (from 0 to 1) and two angles of internal friction (ϕ) were chosen (35° and 40°) to represent medium and dense sand. The depth ratio of topmost layer (u/B) varied (0.25 to 0.65), the vertical distance ratio between consecutive layers of geogrid (h/B) was varied (0.2 to 0.6), and the numbers of geogrid layers were varied (from 1 to 5). Figure (1) shows the major reinforcement parameters of eccentrically loaded strip footing on geogrid reinforced sand.

The term bearing capacity ratio (BCR_e) is presented to express the combined effect of soil reinforcement with load eccentricity on the bearing capacity and it can be written as:

$$BCR_e = \frac{q_{uRe}}{q_u} \quad \ldots\ldots\ldots\ldots\ldots\ldots (1)$$

Where: q_{uRe}: Ultimate bearing capacity of eccentrically loaded strip footing on reinforced sand. q_u: Ultimate bearing capacity of centrically loaded strip footing on unreinforced sand.

Optimum Number of Geogrid Layers

Figure (2) shows the relationship between the bearing capacity ratio (BCR_e) and the eccentricity ratio (e/B) for different number of geogrid layers (N). In this figure it can be noticed that the (BCR_e) significantly increased with the increase of the number of geogrid layers and it decreases with the increase of (e/B). Also it is noticed that there is an optimum value of (N) after which little increase in the value of (BCR_e) is observed, this optimum value is decreased with the increase of eccentricity ratio (e/B). As a result, the optimum values are (N=4) for (e/B=0) and (N=3) for (e/B=0.15).

The effect of depth of footing (D_f /B) on the bearing capacity is shown in Figure (3). It is clear that the ultimate bearing capacity increased with the increase of the depth ratio (D_f /B). Unlike the effect of (N), the depth ratio (D_f /B) has a significant effect on the reduction of the eccentricity ratio (e/B), where increasing the depth ratio (D_f /B) reduced the effect of eccentricity ratio (e/B).

Also Figure (4), shows the effect of the angle of internal friction (ϕ) on the bearing capacity ratio (BCR_e) for different values of eccentricity ratio (e/B). It can be seen that the variation of the angle of internal friction (ϕ) has a little effect on (BCR_e) and almost has no effect on the reduction of eccentricity ratio (e/B).

The effect of the depth ratio of the topmost layer of reinforcement (u/B) on the number of geogrid layers (N) for eccentrically loaded footing is shown in Figure (5). As it can be seen that there is an optimum value of (u/B=0.35) gives the higher values of (BCR_e), as a result, gives the optimum number of geogrid layers (N=3). As increasing the value of (u/B) the value of (BCR_e) is decreased and the optimum number of geogrid is decreased too.

The effect of the vertical distance ratio between consecutive layers (h/B)

on the number of geogrid layers (N) for eccentrically loaded footing is shown in Figure (6). There is minor effect of the value (h/B) on the number of geogrid layers (N) according to the corresponding value of (BCR_e). Also there is an optimum value of (h/B=0.5) which gives an optimum value of (N=3). Furthermore, increasing of the value of (h/B) larger than the optimum is significantly decreases the value of (BCR_e).

Optimum Depth of Topmost Layer

The variation of (BCR_e) with (u/B) for different values of (e/B) are shown in Figure (7). Generally, as the value of (u/B) increased the value of (BCR_e) increased too till it reach a peak value after which a significant decreased of (BCR_e) is noticed. The corresponding value of the peak represents the optimum (u/B) which varied depending on the value of (e/B). For centrically loaded footing the optimum value of (u/B=0.45) which gives the higher value of (BCR_e), this optimum value is decreased with the increase of the eccentricity ratio (i.e. u/B=0.35 for e/B=0.15). Figure (8) shows the effect of depth ratio of the footing (D_f/B) on the value of (u/B) for eccentrically loaded case. It is noticed that the optimum value of (u/B) is increased with the increase of the value of (D_f/B). It should be mentioned that the effect of the depth of embedment (D_f/B) is almost canceling the effect of eccentricity ratio (e/B), this can be attributed to the surcharge load that is caused by the depth of embedment which increases the length of the slip surface and decreases the value of footing tilt. Hence, the stress intensity extended to larger depths than for surface and eccentrically loaded footing. So, the optimum value of (u/B) for embedded and eccentrically loaded footing is increased. Figure (9) shows the effect of the angle of internal friction (ϕ) on the value of (u/B) for eccentrically loaded embedded footing. It is obvious that the variation of (ϕ) has no effect on the optimum value of (u/B) also has a minor effect on the value of (BCR_e). Figure (10) shows the effect of the value of (h/B) on the value of (u/B) for eccentrically loaded footing. It can be seen that the value of (h/B) has no effect on the optimum value of (u/B).

Optimum Vertical Distance between Geogrid Layers

The variation of (BCR_e) with (h/B) for different values of (e/B) are shown in Figure (11). It can be seen that the variation of (e/B) does not influence the value of (h/B) but it certainly reduces the values of (BCR_e) and the optimum value of (h/B=0.5) remains constant.

Figure (12) shows the effect of the depth ratio of the footing (D_f/B) on the value of (h/B) for eccentrically loaded footing. Although increasing the value of (D_f/B) significantly increases the ultimate bearing capacity but it has no effect on the value of (h/B). Figure (13) shows the effect of the angle of internal friction (ϕ) on the value of (h/B) for eccentrically loaded embedded footing. It is noticed that the angle of internal friction has a minor effect on the value of (h/B).

This means that the optimum value of (h/B) is independent on each of the eccentricity ratio (e/B), depth ratio of the footing (D_f/B) and angle of internal friction (ϕ).

Effective Depth Zone of Reinforcement

The effective depth zone of the reinforcement (d) is the depth beneath the footing base, under which no longer

effect of the reinforcement on the bearing capacity is observed. This depth could be calculated as follow:

$$d = u + (N - 1)h \quad \text{……..……..(2)}$$

Where d : effective depth zone of reinforcement. u : depth of first layer of reinforcement beneath the footing base. h : vertical distance between consecutive layers of reinforcement. N : number of geogrid layers. Since the optimum values of (u/B, h/B and N) for centrically loaded footing were found to be (0.45, 0.5 and 4) respectively, the value of effective zone will be ($d \approx 2B$). For eccentrically loaded case (i.e. the eccentricity ratio e/B=0.15), the optimum values of (u/B, h/B and N) are (0.35, 0.5 and 3) respectively, in which the effective depth zone of reinforcement ($d \approx 1.35B$). So that, the effective depth zone (d=1.35B-2B) depending on the load eccentricity and the depth of footing. The concluded value of (d =2B) for centrically loaded case, is the same that concluded by several workers, Das et al. (1994), Shin and Das (2000).

Conclusions

The major conclusions that could be drawn on the behavior of eccentrically loaded strip footing resting on geogrid reinforced sand are outlined below:

(1) The load eccentricity significantly reduces the ultimate bearing capacity of strip footing resting on geogrid reinforced sand and it significantly affects most of the reinforcement parameters.

(2) The results show that increasing the number of geogrid layers (N) significantly increases the ultimate bearing capacity, but there is an optimum value after which little effect is observed. These optimum value are varied (N=3-4) depending on the value of load eccentricity ratio (e/B) and depth of footing (D_f/B).

(3) Increasing the depth of footing (D_f/B) does not affect the optimum value of (N), but it does significantly increase the ultimate bearing capacity and unlike the effect of (N) it has a significant effect on the reduction that is due to the eccentricity ratio (e/B).

(4) Increasing the angle of internal friction (ϕ) increases the ultimate bearing capacity. But it has no effect on the optimum value of (N) or the optimum values of (u/B) and (h/B).

(5) The depth of the first layer (u/B) and the vertical distance between consecutive layers (h/B) have no direct effect on the optimum number of geogrid layers (N).

(6) The optimum value of (u/B) varies (0.35-0.45) depending on the value of eccentricity ratio (e/B) and on the depth ratio of the footing (D_f/B) where it is concluded that the effect of (e/B) and (D_f/B) on (u/B) cancel each other.

(7) The optimum value of the vertical distance between layers is (h/B=0.5) and it is independent on eccentricity ratio (e/B), depth of footing (D_f/B), and the angle of internal friction (ϕ).

(8) The effective depth zone of reinforcement is varied (d/B=1.35-2) depending on the value of eccentricity ratio (e/B) and the value of depth ratio of footing (D_f/B).

References

1. El Sawwaf, M. (2009). "Experimental and Numerical Study of Eccentrically Loaded Strip Footings Resting on Reinforced Sand", Journal of Geotech. and Geoenv. Engrg., Vol. 135, No. 10, pp. 1509-1518.

2. Meyerhof, G. G. (1953). "The Bearing Capacity of Footings under Eccentric and Inclined Loads", Proc. of

3rd Int. Conf. on Soil Mech. and Found. Engrg., Zurich, Vol. 1, 440-444. (Cited by Das 1999)
3. Prakash, S., and Saran, S. (1971). "Bearing Capacity of Eccentrically Loaded Footings", Journal of Soil Mech. and Found. Div., 97(1), 95-118.
4. Purkayastha, R. D., and Char, R. A. (1977). "Stability Analysis for Eccentrically Loaded Footings", Journal of Geotech. Engrg. Div., 103(6), 647-651. (Cited by Das 1999)
5. Binquet, J. and Lee, K. L. (1975a). "Bearing Capacity Tests on Reinforced Earth Slabs", Journal of Geotech. Engrg. Div., ASCE, Vol. 101, No. (12), pp. 1241-1255.
6. Binquet, J. and Lee, K. L. (1975b). "Bearing Capacity Analysis of Reinforced Earth Slabs", Journal of Geotech. Engrg. Div., ASCE, Vol. 101, No. (12), pp. 1257-1276.
7. Huang, C. C., and Tatsuoka, F. (1990). "Bearing Capacity of reinforced Horizontal Sandy Ground", Geotextiles and Geomembranes, Vol. 9, pp. 51-82.
8. Das, B. M., and Omar, M. T. (1994). "The Effect of Foundation Width on Model Tests for the Bearing Capacity of Sand with Geogrid Reinforcement", Geotechnical and Geological Engrg., 12(2), 133-141.
9. Adams, M.T., and Collin, J.G. (1997). "Large Model Spread Footing Load Tests on Geosynthetic Reinforced Soil Foundations", Journal of Geotech. and Geoenv. Engrg. ASCE, Vol. 123, No. 1, pp. 66-72.
10. Huang, C. C., and Menq, F. Y. (1997). "Deep Footing and Wide-Slab Effects on Reinforced Sandy Ground." Journal of Geotech. and Geoenv. Engrg., ASCE, 123 (1), 30-36.
11. Shin, E. C., and Das, B. M. (2000). "Experimental Study of Bearing Capacity of Strip Foundation on Geogrid- Reinforced Sand", Geosynthetics Int., Vol. 7, No. 1, pp. 59-71.
12. Saran, S., Kumar, S., and Kumar, A. (2007). "Analysis of Square and Rectangular Footings Subjected to Eccentric-Inclined Load Resting on Reinforced Sand", Journal of Geotechnical and Geological Engrg., 25, 123-137.
13. Patra, C. R., Das B. M., Bhoi, M. and Shin, E. C. (2006). "Eccentrically Loaded Strip Foundation on Geogrid-Reinforced Sand", Journal of Geotextiles and Geomembranes, 24(4), 254-259.
14. Al-Taay, A. H. (2010). "Bearing Capacity of Eccentrically Loaded Strip Footing on Geogrid Reinforced Sand". M.Sc. Thesis, Tikrit University, Iraq.
15. Bowles, J. E. (1996). "Foundation Analysis and Design", 5th Edition, McGraw-Hill Book Co. New York.
16. PLAXIS b.v. Software manual. (2002). "Scientific Manual", A.A. Balkema Publishers. Tokyo.

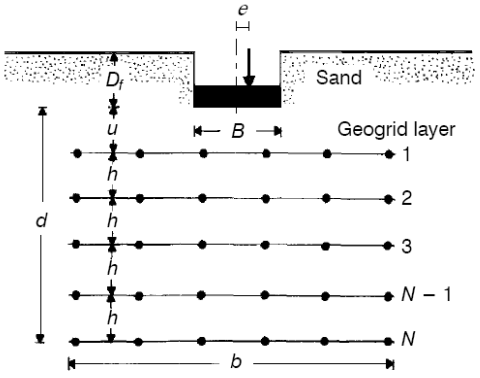

Figure (1) Eccentrically loaded strip footing on geogrid-reinforced sand

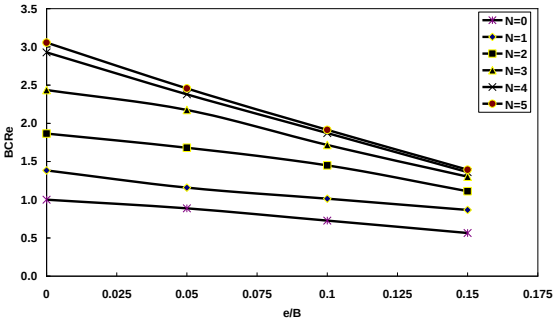

Figure (2): (BCR_e)-(e/B) relationship for different (N)
(D_f /B=0, u/B=0.45, h/B=0.5, $\phi = 35^\circ$)

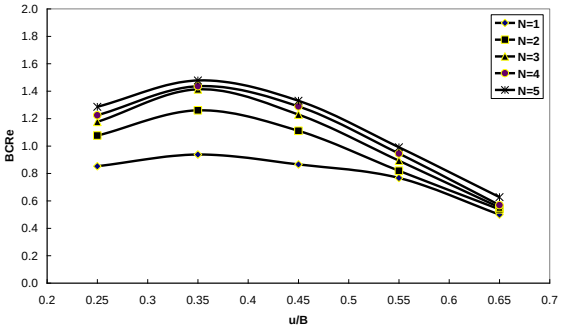

Figure (5): (BCR_e)-(u/B) relationship for different (N)
(e/B=0.15, h/B=0.5, D_f /B=0.5, $\phi = 35^\circ$)

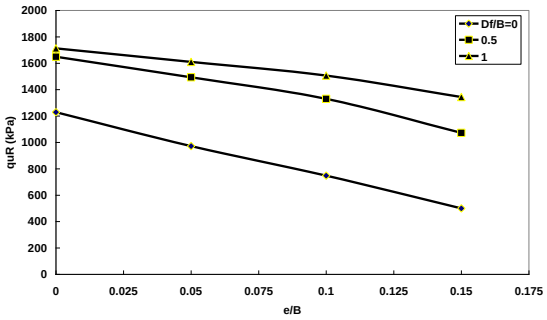

Figure (3):(e/B)-(q_{uR}) relationship for different (D_f /B)
(N=4, u/B=0.45, h/B=0.5, $\phi = 35^\circ$)

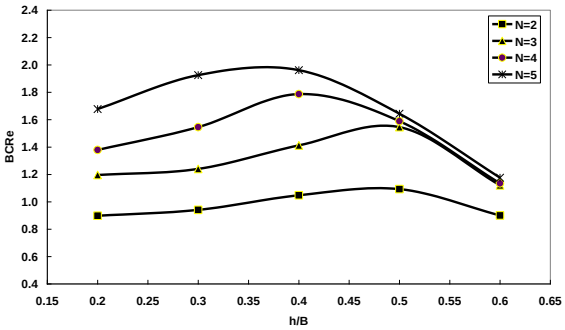

Figure (6):(BCR_e)-(h/B) relationship for different (N) for
(e/B=0.15, D_f /B=0.5, u/B=0.45, $\phi = 35^\circ$)

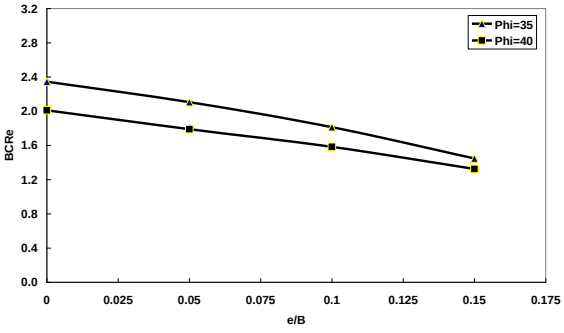

Figure (4): (BCR_e)-(e/B) relationship for different (ϕ)
(N=4, u/B=0.45, h/B=0.5, D_f /B=0.5)

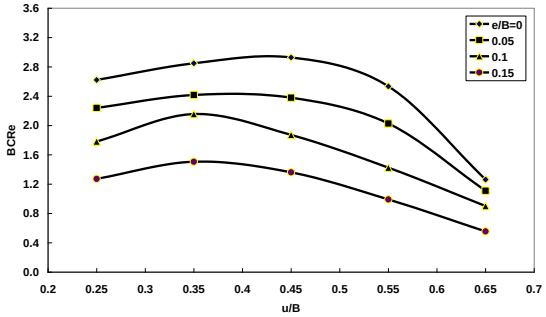

Figure (7): (BCR_e)- (u/B) relationship for different (e/B)
(D_f /B=0, N=4, h/B=0.5, $\phi = 35^\circ$)

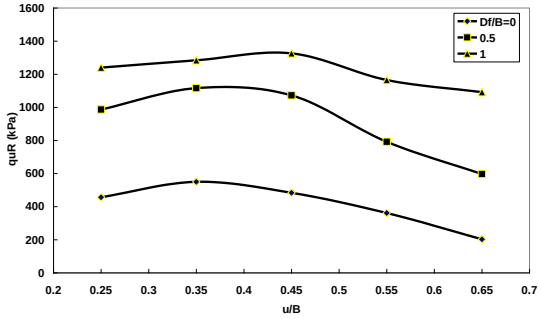

Figure (8): (q_{uR})- (u/B) relationship for different (D_f /B)
(e/B=0.15, N=4, h/B=0.5, $\phi = 35^\circ$)

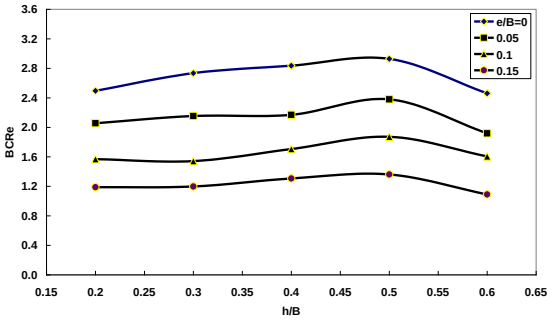

Figure (11): (BCR_e)-(h/B) relationship for different (e/B)
(D_f /B=0, N=4, u/B=0.45, $\phi = 35^\circ$)

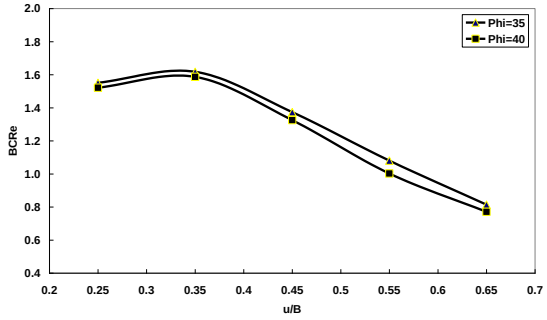

Figure (9): (BCR_e)- (u/B) relationship for different (ϕ) for
(e/B=0.15, D_f /B=0.5, N=4, h/B=0.5)

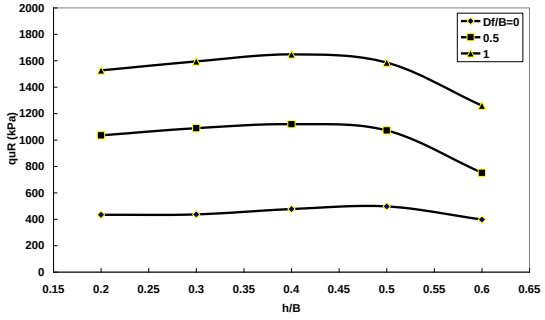

Figure (12): (q_{uR})-(h/B) relationship for different (D_f /B)
(e/B=0.15, N=4, u/B=0.45, $\phi = 35^\circ$)

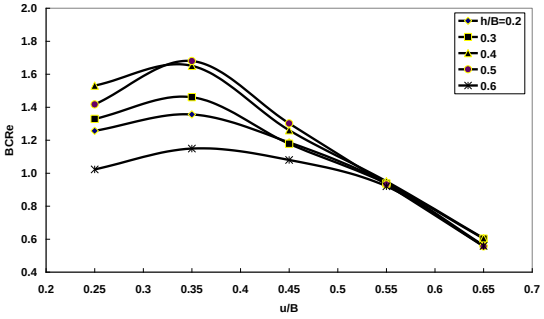

Figure (10): (BCR_e)- (u/B) relationship for different (h/B) for
(e/B=0.15, D_f /B=0, N=3, $\phi = 35^\circ$)

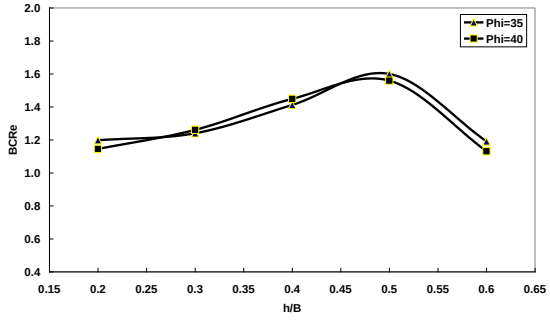

Figure (13): (BCR_e)-(h/B) relationship for different (ϕ)
(e/B=0.15, D_f /B=0.5, N=4, u/B=0.45)

Table (1) Soil parameters used in the present study

Parameter	Medium desnse sand	Dense sand
E_{50} (kN/m^2)*	35000	50000
ϕ ($^\circ$)	35	40
(c) (kN/m^2)	1	1
(v)*	0.3	0.35
fψ ($^\circ$) **	5	10
γ (kN/m^3)	16.5	17.5
(R_{int})**	1.0	1.0

Table (2) Footing and geogrid parameters

Parmeter	Footing **	Geogrid***
EI ($kN.m^2/m$)	5000000	-
EA (kN/m)	8500	2000

* These values are Chosen after Bowles (1996)[15]
** Chosen after Plaxis scientific Manual (2002)[16]
*** Chosen after El-Sawaf (2009)[1]

Table (3) Engineering properties of Tenax TT Samp geogrid

Structure	Mono-oriented geogrid
aperture shape	oval apertures
aperture size (*mm*×*mm*)	(13/20)×220
weight (gm/m^2)	300
polymer type	HDPE
tensile strength @ 2% strain (kN/m)	11
tensile strength @ 5% strain (kN/m)	25
peak tensile strength (kN/m)	45
yield point elongation (%)	11.5
long term design strength (kN/m)	21.2